Antenna Design Concepts Based on Transformation Electromagnetics Approach

Paul-Henri TICHIT[1], Shah Nawaz BUROKUR[1,2], André de LUSTRAC[1,2]

[1] IEF, Univ. Paris-Sud, CNRS, UMR 8622, 91405 Orsay cedex, France
[2] Univ. Paris-Ouest, 92410 Ville d'Avray, France

paul-henri.tichit@u-psud.fr, shah-nawaz.burokur@u-psud.fr, andre.de-lustrac@u-psud.fr

Abstract. *Using the idea of wave manipulation via coordinate transformation, we demonstrate the design of novel antenna concepts. The manipulation is enabled by composite metamaterials that realize the space coordinate transformation. We present the design, realization and characterization of three types of antennas: a directive, a steered beam and a quasi-isotropic one. Numerical simulations together with experimental measurements are performed in order to validate the concept. Near-field cartography and far-field pattern measurements performed on a fabricated prototype agree qualitatively with Finite Element Method (FEM) simulations. It is shown that a particular radiation can be transformed at ease into a desired one by modifying the electromagnetic properties of the space around it. This idea can find various applications in novel antenna design techniques for aeronautical, telecommunication and transport domains.*

Keywords

Antennas, metamaterials, transformation electromagnetics.

1. Introduction

Metamaterials have recently attracted considerable interests because of their capabilities which go beyond conventional materials and because of their applications in novel class coordinate transformation (also called transformation optics or in a more general way transformation electromagnetics) based devices. The concept of transformation electromagnetics was first proposed by J. B. Pendry [1] and U. Leonhardt [2] in 2006. It is a powerful mathematical tool used to generate a new transformed space from an initial one where solutions of Maxwell's equations are known by manipulating electromagnetic waves. It provides the conceptual design of novel, and otherwise unattainable, electromagnetic and optical devices by controlling the paths of wave propagation. The first example of this successful merging was the design and experimental characterization of an invisibility cloak in 2006 [3]. Other interesting wave manipulation applications such as wave concentrators [4], field rotators [5], electromagnetic wormholes [6], waveguide transitions and bends [7-11] have also been proposed. Concerning antenna applications, focusing lens antennas [12-14] and the engineering of radiation patterns [15] have been proposed. The performances of an omnidirectional retroreflector [16] based on the transmutation of singularities [17] and Luneberg lenses [18] have also been experimentally demonstrated. An octave-bandwidth horn antenna has experimentally validated for satellite communications [19].

Recent techniques of source transformation [20-22] have offered new opportunities for the design of active devices with source distribution included in the transformed space. This approach has led us to design an ultra-directive emission by stretching a source into an extended coherent radiator [23-25]. The design has been implemented through the use of judiciously engineered metamaterials and the device is shown experimentally to produce an ultra-directive emission. This idea has been extended to a second device, a wave bending one, so as to achieve a steered beam antenna via a rotational coordinate transformation [26]. Experimental measurements have shown a beam steering as much as 66°. Finally, a quasi-isotropic emission is numerically designed from a directive source by performing a space expansion [27].

2. Directive Antenna

The design of the directive antenna is based on the transformation of a cylindrical space into a rectangular one. The schematic principle of the transformation is presented in Fig. 1(a). The theoretical underlying physics of the transformation involved here has been detailed recently in [23]. The concept is as follows: the imagined space of our proposed antenna is obtained by transforming a flat isotropic cylindrical half-space with zero Riemann curvature tensor described in polar coordinates $\{r, \theta\}$ into a flat space in squeezed Cartesian coordinates. x', y' and z' are the coordinates in the virtual transformed rectangular space and x, y, z are those in the initial real cylindrical space. In the theoretical study of [23], we have shown that the coordinate transformation can be implemented by a material obeying the tensors:

$$\psi^{i'j'} = g^{i'j'}\left|\det\left(g^{i'j'}\right)\right|^{-\frac{1}{2}}\psi \tag{1}$$

where ψ represents the permittivity or permeability tensor and g the metric tensor of our designed space. The material must then be able to produce the following dielectric tensors presenting no non-diagonal components:

$$\varepsilon^{ij} = \mu^{ij} = diag\left(\varepsilon_{xx}(x'), \frac{1}{\varepsilon_{xx}(x')}, \alpha\varepsilon_{xx}(x')\right) \tag{2}$$

where $\varepsilon_{xx}(x') = \frac{\pi x'}{e}$ and $\alpha = \frac{d^2}{4L^2}$. d represents the diameter of the initial cylindrical space and e and L, respectively the width and length of the rectangular target space.

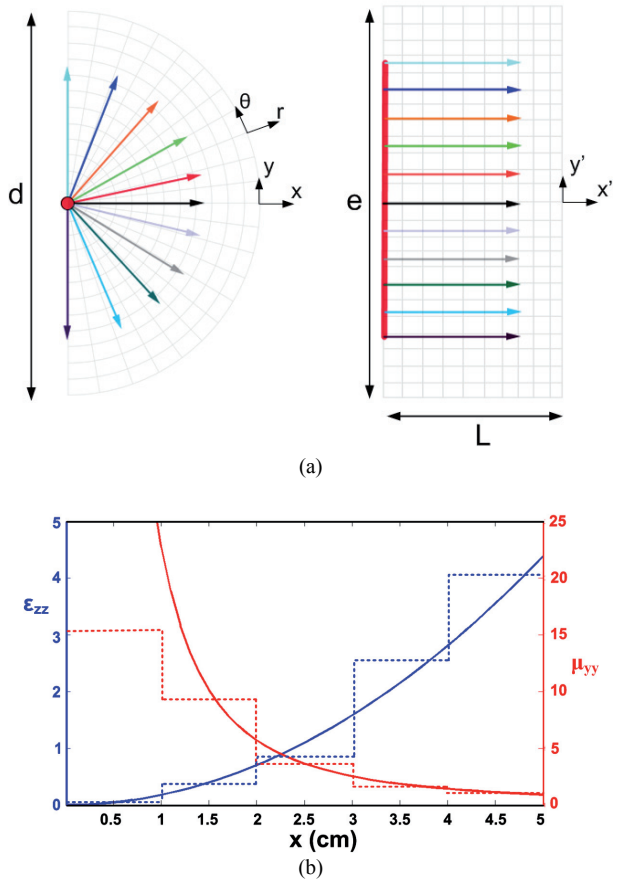

Fig. 1. (a) Transformation of a cylindrical space into a rectangular one. (b) Continuous (continuous lines) and discretized (dashed lines) variations of permeability and permittivity of the material.

For a practical implementation using metamaterials, the dimensions of the semi-cylindrical space is set so that $\alpha = 4$ in order to obtain achievable values for the electromagnetic parameters. Additional simplification arises from the choice of the polarization of the emitted wave. Here, we consider a polarized electromagnetic wave with an electric field pointing in the z-direction, which allows modifying the dispersion equation in order to simplify the electromagnetic parameters without changing Maxwell's equations and propagation in the structure. This leads to a metamaterial which is described with $e = 0.15$ m and $L = 0.05$ m by:

$$\mu_{xx} = 1 \;;\; \mu_{yy} = \frac{1}{(\varepsilon_{xx})^2} \;;\; \varepsilon_{zz} = 4(\varepsilon_{xx})^2. \tag{3}$$

Discrete values are then created for the desired variation of μ_{yy} and ε_{zz} to secure a practical realization producing experimental performances close to theory, as illustrated in Fig. 1(b). Fig. 2 shows a photography of the fabricated prototype. A microstrip square patch antenna printed on a 0.787 mm thick low-loss dielectric substrate (Rogers RT/Duroid 5870TM with 17.5 µm copper cladding, $\varepsilon_r = 2.33$ and $\tan\delta = 0.0012$) is used as radiating source. A surrounding material made of alternating electric metamaterial and magnetic metamaterial layers transforms the isotropic emission of the patch antenna into a directive one. The metamaterial is a discrete structure composed of five different regions where permittivity and permeability vary according to (3) and to the profile of Fig. 1(b).

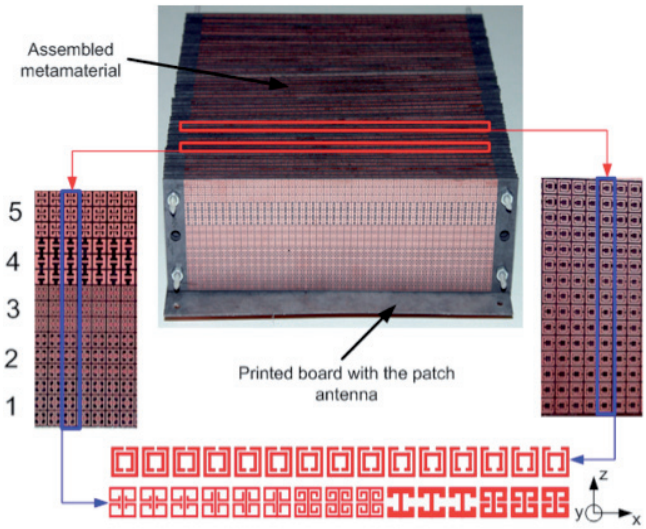

Fig. 2. Photography of the structure of the antenna. The inserts show the permittivity (left) and the permeability (right) layers of the material.

The axial permittivity ε_{zz} and permeability μ_{yy} show respectively values ranging from 0.12 to 4.15 and from 1.58 to 15.3. The bulk metamaterial is assembled using 56 layers of dielectric boards on which subwavelength resonant structures are printed. 28 layers contain split ring resonators (SRRs) [28] and 28 others contain electric-LC resonators (ELCs) [29], shown by the insets of Fig. 2. Such structures are known to provide respectively a magnetic and an electric response. Each layer is made of 5 regions of metamaterials corresponding to the discretized values of Fig. 1(b). Because of constraints of the layout, we choose a rectangular unit cell with dimensions 3.333 mm for both resonators. The layout consists of 5 regions, each of which is three unit cells long (10 mm). We are able to obtain the desired μ_{yy} and ε_{zz} by tuning the resonators' geometric

parameters. Details concerning the SRR and ELC resonators are given in Fig. 3. The resonators are simulated using finite-element method based Ansys HFSS commercial code in the [8 GHz – 15 GHz] frequency band. The effective material parameters μ_{yy} and ε_{zz} are then retrieved from the calculated S-parameters, through the use of a retrieval process described in [30]. μ_{yy} and ε_{zz} are respectively shown in Fig. 4(a) and 4(b). The insets of Fig. 4 show the variation of the two material parameters in the vicinity of 10 GHz.

SRR

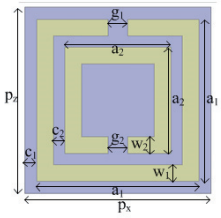

region	a_2	c_2	g_1	g_2	μ_{yy}
1	1.9	0.2	0.35	0.35	15.3
2	1.9	0.2	0.38	0.38	10
3	1.8	0.25	0.36	0.3	3.66
4	1.8	0.25	0.8	0.6	1.89
5	1.8	0.25	1.2	0.6	1.58

$p_x = p_z = 10/3$, $a_1 = 2.9$, $w_1 = w_2 = 0.3$, $c_1 = 0.2165$

ELC

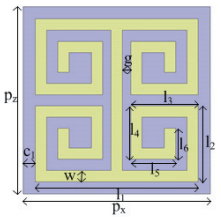

region	l_4	l_5	l_6	ε_{zz}
1	0.5	0	0	0.15
2	0.9	0	0	0.4
3	0.95	0.8	0.55	0.65

$p_x = p_z = 10/3$, $l_1 = 2.9$, $l_2 = 1.35$, $l_3 = 1.2$, $w = 0.2$, $g = 0.15$, $c_1 = 0.2165$

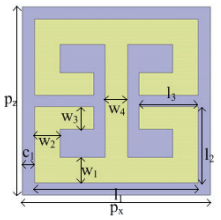

region	l_2	l_3	w_3	ε_{zz}
4	1	0	0	2.74
5	1.35	1.05	0.4	4.15

$p_x = p_z = 10/3$, $l_1 = 2.9$, $w_1 = w_2 = 0.6$, $w_4 = 0.4$, $c_1 = 0.2165$

All dimensions are in mm.

Fig. 3. Unit cell of the SRR used as magnetic material and of the ELC used as electric material. The tables summarize the dimensions of these two metamaterial cells to achieve the different values of the electromagnetic parameters needed for the transformation.

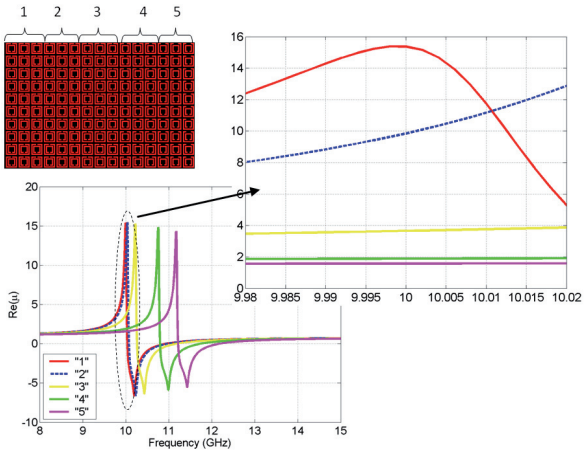

(a)

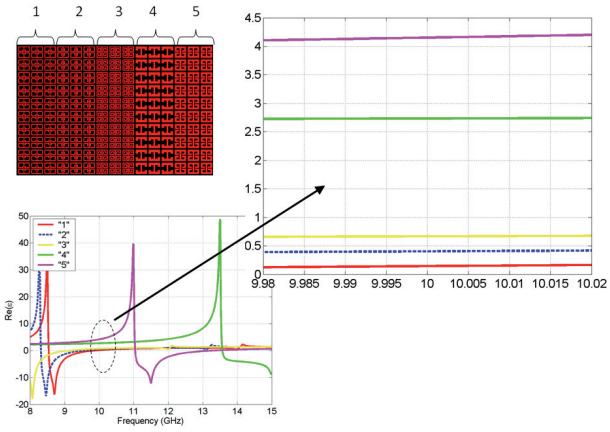

(b)

Fig. 4. (a) Magnetic response of the SRR for the 5 regions. (b) Electric response of the ELC for the 5 regions.

The layers are mounted 2 by 2 with a constant air spacing of 2.2 mm between each. Overall dimensions of our antenna are 15 cm x 15 cm x 5 cm. The E-plane radiation patterns have been measured and compared to the calculated ones at 10.6 GHz (Fig. 5). The metamaterial-based antenna is used as emitter and a wideband [2 GHz to 18 GHz] is used as receiver. A good agreement is observed. The transformation of the patch's omnidirectional radiation into a directive is clearly established. A narrow half-power beamwidth of 13° is observed for the measured antenna. These performances are competitive with classical high directivity antennas such as parabolic reflector antennas.

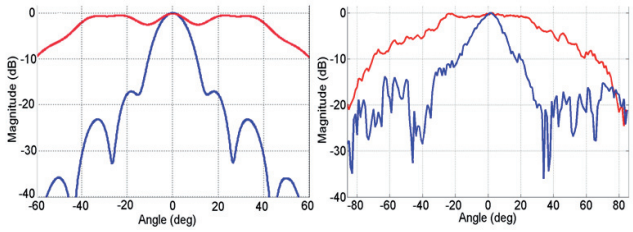

Fig. 5. (a) Calculated and (b) measured radiation pattern at 10.6 GHz of the proposed metamaterial antenna (blue) and the microstrip patch radiator alone (red).

3. Steered Beam Antenna

In this section, we propose a two-dimensional coordinate transformation, which transforms the vertical radiation of a plane source into a directive azimuthal emission. Let us consider a source radiating in a rectangular space. Theoretically this radiation emitted from the latter source can be transformed into an azimuthal one using transformation optics. The transformation procedure is noted $F(x',y')$ and consists in bending the emission. Fig. 6 shows the working principle of this rotational coordinate transformation. Mathematically, $F(x',y')$ can be expressed as [26]:

$$\begin{cases} x' = ax\cos(by) \\ y' = ax\sin(by) \\ z' = z \end{cases} \tag{4}$$

where x', y', and z' are the coordinates in the bent space, and x, y and z are those in the initial rectangular space. In the initial space, we assume free space. L_2-L_1 and L are respectively the width and the length of the rectangular space. The rotational transformation of Fig. 6 is defined by a considered as an "expansion" parameter and b which controls the rotation angle of the transformation $F(x',y')$.

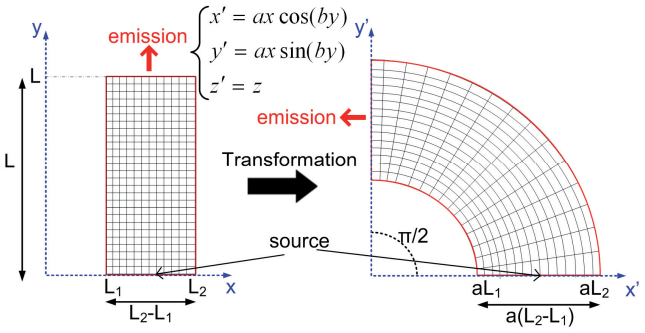

Fig. 6. Schematic illustration of the 2D transformation: (a) Initial rectangular space, (b) transformed space.

By substituting the new coordinate system in the tensor components, and after some simplifications, the material parameters are derived in the diagonal base:

$$\overline{\overline{\psi}} = \begin{pmatrix} \psi_{xx} & \psi_{xy} & 0 \\ \psi_{yx} & \psi_{yy} & 0 \\ 0 & 0 & \psi_{zz} \end{pmatrix}$$

$$\text{with} \begin{cases} \psi_{xx} = \dfrac{a^2x'^2 + b^2y'^2r^2}{abr^3} \\ \psi_{xy} = \psi_{yx} = \dfrac{x'y'\left(a^2 - b^2r^2\right)}{abr^3} \\ \psi_{yy} = \dfrac{a^2y'^2 + b^2x'^2r^2}{abr^3} \\ \psi_{zz} = \dfrac{1}{abr} \end{cases} \tag{5}$$

Fig. 7 shows the variation of the different components of the permeability and the permittivity tensor of the metamaterial structure. The geometrical dimensions are as follows: the width of the source is taken to be 5 cm, and the internal and external radius of the metamaterial structure is respectively 5 cm and 10 cm. The working frequency is set to 10 GHz.

After diagonalization, calculations lead to permeability and permittivity tensors given in the diagonal base by:

$$\overline{\overline{\varepsilon}} = \begin{pmatrix} \psi_{rr} & 0 & 0 \\ 0 & \psi_{\theta\theta} & 0 \\ 0 & 0 & \psi_{zz} \end{pmatrix} \varepsilon_0$$

$$\overline{\overline{\mu}} = \begin{pmatrix} \psi_{rr} & 0 & 0 \\ 0 & \psi_{\theta\theta} & 0 \\ 0 & 0 & \psi_{zz} \end{pmatrix} \mu_0 \tag{6}$$

with:

$$\psi_{rr} = \frac{a}{br}; \psi_{\theta\theta} = \frac{a}{b}r; \psi_{zz} = \frac{1}{abr} \tag{7}$$

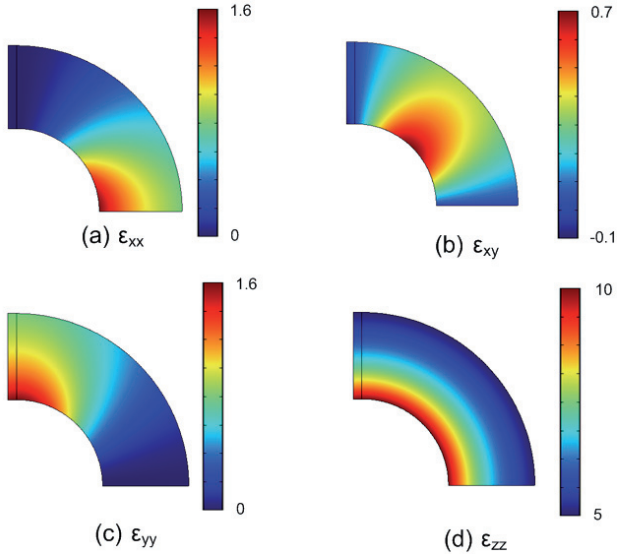

Fig. 7. Variation of the permittivity tensor components: (a) ε_{xx}, (b) ε_{xy}, (c) ε_{yy}, (d) ε_{zz}.

The transformation formulation is implemented using FEM method based commercial solver Comsol Multiphysics. Fig. 8 shows the comparison of 2D simulations between a plane source made of current lines in yz plane above a limited metallic ground plane (Fig. 8(a)) and the same source surrounded by a metamaterial defined by (7), Fig. 8(b). Fig. 8(c) and 8(d) show respectively the far-field patterns of the plane source without and with the metamaterial structure. The left shift of the peak corresponds to a rotation of 76° of the emitted radiation.

For a physical prototype fabrication, we need to simplify the calculated material parameters through a parameter reduction procedure. We therefore set a polarization of the electromagnetic field such that the magnetic field is along the z-direction. In this case, the relevant electromagnetic parameters are μ_{zz}, $\varepsilon_{\theta\theta}$ and ε_{rr}. We maintain $\varepsilon_{\theta\theta}$ and μ_{zz} constant and hence the new set of coordinates is given by (8):

$$\varepsilon_{rr} = \left(\frac{1}{br}\right)^2 \div 1.7; \varepsilon_{\theta\theta} = 2.8; \mu_{zz} = 1.7 \tag{8}$$

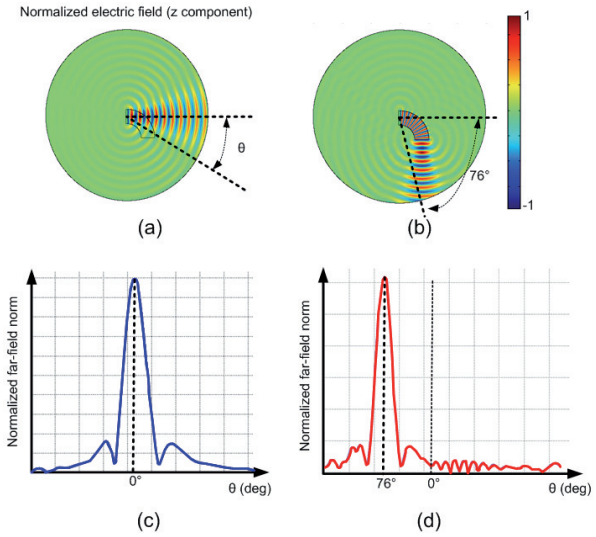

Fig. 8. (a)-(b) Calculated emission of a plane current source above a limited metallic ground plane without and with the metamaterial structure. (c)-(d) Calculated normalized far field of the antenna without and with metamaterial. A 76° rotation of the radiation is clearly observed.

Setting physical parameter $b = 6$ allows an optimization of the material parameter ε_{rr}. The continuous profile of the different parameters is presented in Fig. 9(a). The fabricated prototype is considered to be composed of 30 identical layers where each layer is divided in 10 unit cells as illustrated in Fig. 9(b). The cells are composed of respectively SRRs [28] and ELCs [29] to secure μ_{zz} and ε_{rr}. $\varepsilon_{\theta\theta}$ is produced by a host medium, which is a commercially available resin. The meta-atoms are designed on a 0.787 mm thick low loss ($\tan\delta = 0.0013$) RO3003^{TM} dielectric substrate. We choose a rectangular unit cell with dimensions 5 mm for the resonators. We are able to obtain the desired ε_{zz} and μ_{yy} by tuning the resonators' geometric parameters. The 10 cells presented in Fig. 9(c) are designed to constitute the discrete variation of ε_{rr}. Tab. 1 summarizes the corresponding electromagnetic parameters of the cells.

Layer	r_i (mm)	$L_{\theta i}$ (mm)	μ_{zz}	ε_{rr}
1	52.5	2.75	1.7	5.8
2	57.5	3.01	1.7	4.84
3	62.5	3.27	1.7	4.1
4	67.5	3.53	1.7	3.5
5	72.5	3.8	1.7	3.04
6	77.5	4.06	1.7	2.66
7	82.5	4.32	1.7	2.35
8	87.5	4.58	1.7	2.09
9	92.5	4.84	1.7	1.87
10	97.5	5.1	1.7	1.68

Tab. 1. Electromagnetic parameters μ_{zz}, and ε_{rr} for the 10 cells of the metamaterial layers. The length L_θ of each cell is given as a function of its position along the layer.

For numerical verifications of the proposed device performances, a microstrip patch antenna presenting a quasi-omnidirectional radiation is used as the feeding source of the metamaterial antenna. This patch source is optimized for a 10 GHz operation. A 3D simulation of the patch antenna and the layered metamaterial is performed using ANSYS commercial electromagnetic solver HFSS as illustrated in Fig. 10(a). Fig. 10(b) shows the calculated energy distribution in the middle plane of the layered metamaterial structure. We shall note that the latter structure firstly transforms the quasi-omnidirectional radiation of the patch source into a directive one and also maintains this highly directive emission after the 76° rotation.

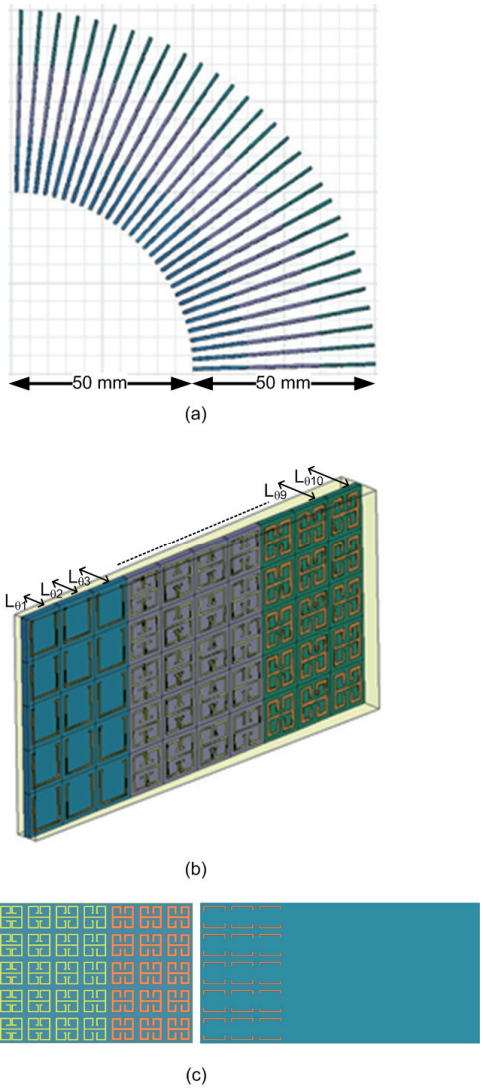

Fig. 9. (a) Profile of the material parameters. (b) Single metamaterial layer composed of 10 unit cells providing the material parameters necessary for the coordinate transformation. (c) Front and rear view of the metamaterial cells.

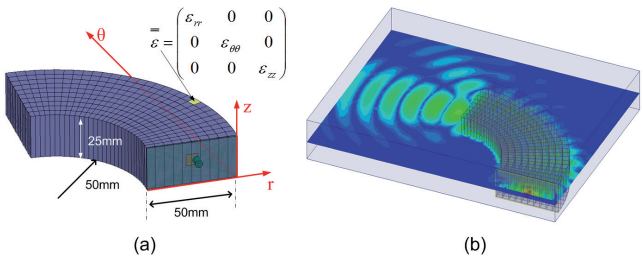

Fig. 10. (a) Simulated design consisting of 30 metamaterial layers each composed of 10 cells. (b) Calculated energy distribution at 10 GHz.

For the fabrication of the device, a microstrip square patch antenna printed on a 1 mm thick epoxy dielectric substrate ($\varepsilon_r = 3.9$ and $\tan\delta = 0.02$) is used as radiating source. The metamaterial is a discrete structure composed of 10 different regions where permittivity and permeability vary according to (8) and to the values of Tab. 1. The bulk metamaterial is assembled using 30 layers of RO3003^{TM} dielectric boards on which subwavelength resonant structures are printed. The layers are mounted 1 by 1 in a molded matrix with a constant angle of 3° between each. A commercially available liquid resin is then flowed into the mold. This resin constitutes the host medium and is an important design parameter which is closely linked to $\varepsilon_{\theta\theta}$. Its measured permittivity is close to 2.8. The mold is then removed after solidification of the resin.

To validate experimentally the fabricated steered directive emission device shown in Fig. 11(a), S_{11} parameter measurements are first performed and compared with the HFSS-simulated one in Fig. 11(b). A good agreement can be observed and return losses reaching 18 dB is observed experimentally at 10.3 GHz compared to 15 dB calculated. This quantity is further compared with that of the feeding patch antenna alone. A better matching can be clearly observed for the metamaterial antenna. The E-plane far-field radiation pattern of the metamaterial antenna is measured in a fully anechoic chamber. Measurements are performed for computer-controlled elevation angle varying from -90° to +90°. The measured far-field radiation pattern is presented for the metamaterial device (Fig. 11(c)). From the experiments, we can clearly observe the transformation of the omni-directional far-field radiation of the patch antenna into a directive one which is further bent at an angle of 66°, which is consistent to the 76° predicted by numerical simulations. The difference in bending angle is due to the fabrication tolerances of the meta-atoms providing the gradient radial permittivity and to the positioning of the patch source.

4. Isotropic Antenna

Conversely to the previous sections where we dealt with directive beams obtained from omnidirectional sources, here we focus our attention on how coordinate transformation can be applied to transform directive emissions into isotropic ones. An intuitive schematic principle to illustrate the proposed method is presented in Fig. 12. Let us consider a source radiating in a circular space as shown in Fig. 12(a) and a circular region bounded by the blue circle around this source limits the radiation zone. The "space stretching" coordinate transformation consists in stretching exponentially the central zone of this delimited circular region represented by the red circle as illustrated in Fig. 12(b).

The expansion procedure is further followed by a compression of the annular region formed between the red and blue circles so as to secure a good impedance matching with free space. Fig. 12(c) summarizes the expo-

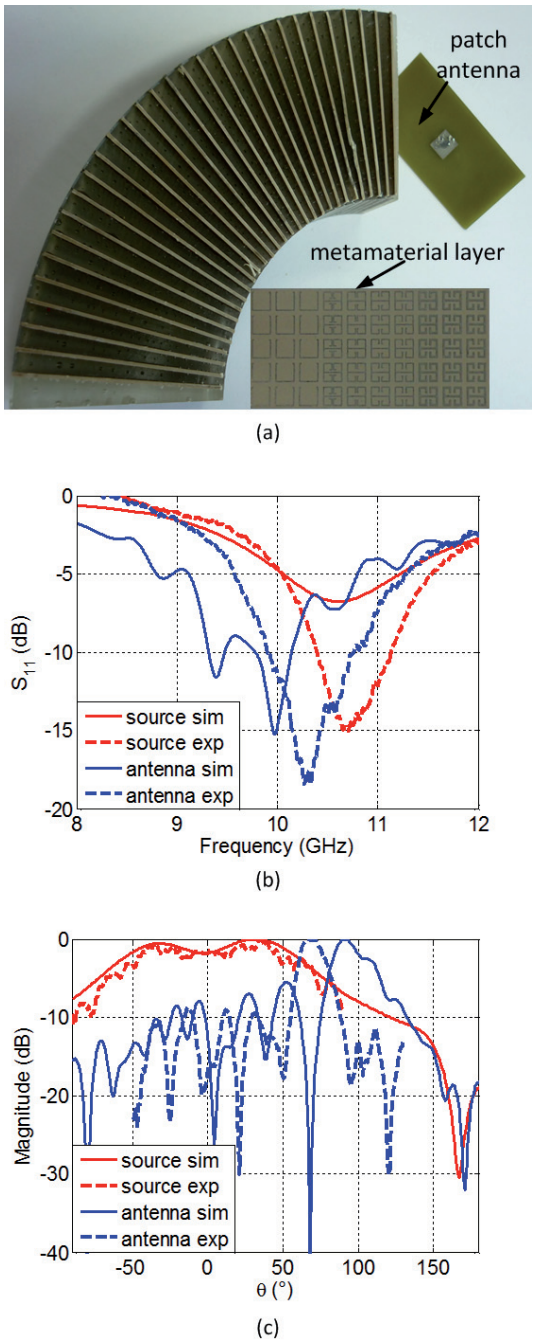

Fig. 11. (a) Photography of the fabricated metamaterial-based prototype. (b) Simulated and measured S_{11} parameter of the patch source alone and the metamaterial antenna. (c) Far-field E-plane radiation patterns of the patch source alone and of the metamaterial antenna.

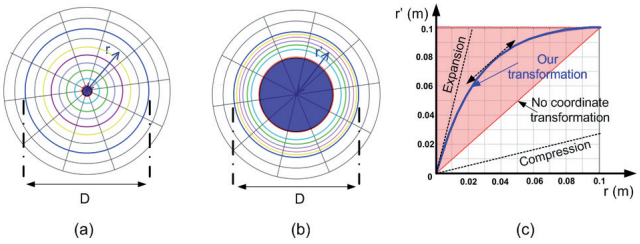

Fig. 12. (a) Initial space, (b) transformed space, (c) the blue curve shows the transformation rule made of an expansion followed by a compression.

nential form of our coordinate transformation. The diameter of the transformed (generated metamaterial) circular medium is noted D.

Mathematically this transformation is expressed as [27]:

$$\begin{cases} r' = \alpha(1 - e^{qr}) \\ \theta' = \theta \\ z' = z \end{cases} \quad \text{with} \quad \alpha = \frac{D}{2}\frac{1}{1 - e^{\frac{qD}{2}}} \tag{9}$$

where r', θ', and z' are the coordinates in the transformed cylindrical space, and r, θ, and z are those in the initial cylindrical space. In the initial space, we assume free space, with isotropic permittivity and permeability tensors ε_0 and μ_0. Parameter q (in m^{-1}) appearing in (9) must be negative in order to secure the impedance matching condition. This parameter is an expansion factor which can be physically viewed as to what extent space is expanded. A high (negative) value of q means a high expansion whereas a low (negative) value of q means a nearly zero expansion.

Calculations lead to permeability and permittivity tensors given in the diagonal base by:

$$\overline{\overline{\psi}} = \begin{pmatrix} \psi_{rr} & 0 & 0 \\ 0 & \psi_{\theta\theta} & 0 \\ 0 & 0 & \psi_{zz} \end{pmatrix} = \begin{pmatrix} \frac{qr(r'-\alpha)}{r'} & 0 & 0 \\ 0 & \frac{r'}{qr(r'-\alpha)} & 0 \\ 0 & 0 & \frac{r}{r'q(r'-\alpha)} \end{pmatrix}$$

with:
$$r = \frac{\ln\left(1 - \frac{r'}{\alpha}\right)}{q}. \tag{10}$$

The components in the Cartesian coordinate system are calculated and are as follows:

$$\begin{cases} \psi_{xx} = \psi_{rr}\cos^2(\theta) + \psi_{\theta\theta}\sin^2(\theta) \\ \psi_{xy} = \psi_{yx} = (\psi_{rr} - \psi_{\theta\theta})\sin(\theta)\cos(\theta) \\ \psi_{yy} = \psi_{rr}\sin^2(\theta) + \psi_{\theta\theta}\cos^2(\theta) \end{cases} \tag{11}$$

By fixing the electric field directed along the z-axis and by adjusting the dispersion equation without changing propagation in the structure, the following reduced parameters can be obtained:

$$\begin{cases} \mu_{rr} = 1 \\ \mu_{\theta\theta} = \left(\frac{r'}{qr(r'-\alpha)}\right)^2 \\ \varepsilon_{zz} = \left(\frac{r}{r'}\right)^2 \end{cases} \tag{12}$$

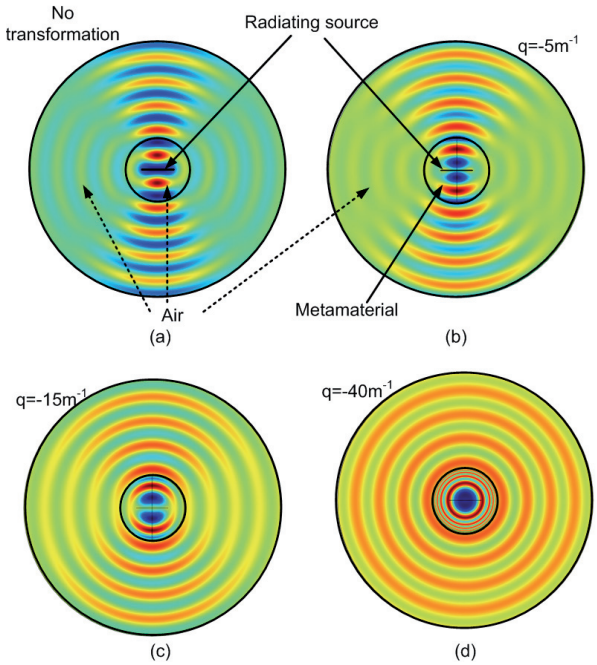

Fig. 13. Simulated electric field distribution for a TE wave polarization at 4 GHz. (a) Current plane source used as excitation for the transformation. The current direction is perpendicular to the plane of the figure; (b)-(d) Verification of the transformation for different values of expansion factor q.

Fig. 13 presents simulations results of the source radiating in the initial circular space at an operating frequency of 4 GHz for several values of q. The current direction of the source is supposed to be along the z-axis. Simulations are performed in a Transverse Electric (TE) mode with the electric field polarized along z-direction. The surface current source is considered to have a width of 10 cm, which is greater than the 7.5 cm wavelength at 4 GHz. Radiation boundary conditions are placed around the calculation domain in order to plot the radiation properties. Continuity of the field is assured in the interior boundaries. As stated previously and verified from the different electric field distribution patterns, a high negative value of q leads to a quasi-perfect isotropic emission since the space expansion is higher. This phenomenon can be clearly observed in Fig. 13(d) for q = -40 m^{-1}.

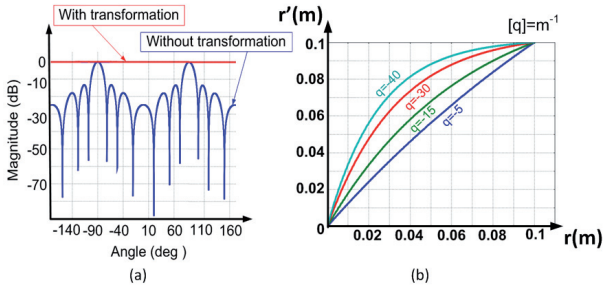

Fig. 14. (a) Far field radiation pattern of the emission with (q = -40 m^{-1}) and without transformation. (b) Influence of the expansion parameter q on the proposed coordinate transformation. The emitted radiation is more and more isotropic as q tends to high negative values.

The calculated far-field patterns are shown in Fig. 14(a). The source alone produces a directive emission and when it is surrounded by the judiciously engineered coordinate-transformation based metamaterial, an isotropic emission is produced. Fig. 14(b) shows the influence of parameter q on the space expansion in the coordinate transformation. As q becomes highly negative, a greater space expansion is achieved.

A possible prototype of our proposed transformation-based isotropic device is presented in Fig. 15 where permeability and permittivity metamaterial layers are used to assure both $\mu_{\theta\theta}$ and ε_{zz} gradient. Here the material is composed of permittivity and permeability alternated layers disposed radially around the central directive antenna. These layers are made of metamaterials as for the directive antenna.

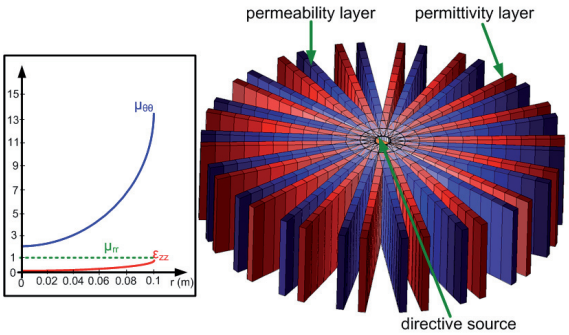

Fig. 15. Schematic structure of the antenna. Schematic of a possible prototype with tailored permittivity and permeability values in a cylindrical configuration.

5. Conclusion

To summarize, recent techniques of source transformation have offered new opportunities for the design of radiating devices with source distribution included in the transformed space. This approach has led us to design an ultra-directive emission by stretching a source into an extended coherent radiator and also a quasi-isotropic emission from a directive source by space expansion. We have also designed a beam steerable antenna by using a rotational coordinate transformation. Experimental measurements performed on the directive and beam steerable antennas have shown concluding results, making these devices compatible for aeronautical and transport domains.

References

[1] PENDRY, J. B., SCHURIG, D., SMITH, D. R. Controlling electromagnetic fields. *Science*, 2006, vol. 312, no. 5781, p. 1780 to 1782.

[2] LEONHARDT, U. Optical conformal mapping. *Science*, 2006, vol. 312, no. 5781, p. 1777-1780.

[3] SCHURIG, D., MOCK, J. J., JUSTICE, B. J., CUMMER, S. A., PENDRY, J. B., STARR, A. F., SMITH, D. R. Metamaterial electromagnetic cloak at microwave frequencies. *Science*, 2006, vol. 314, no. 5801, p. 977-980.

[4] RAHM, M., SCHURIG, D., ROBERTS, D. A., CUMMER, S. A., SMITH, D. R., PENDRY, J. B. Design of electromagnetic cloaks and concentrators using form-invariant coordinate transformations of Maxwell's equations. *Photonics and Nanostructures – Fundamentals and Applications*, 2008, vol. 6, no. 1, p. 87-95.

[5] CHEN, H., HOU, B., CHEN, S., AO, X., WEN, W., CHAN, C. T. Design and experimental realization of a broadband transformation media field rotator at microwave frequencies. *Physical Review Letters*, 2009, vol. 102, no. 18, p. 183903.

[6] GREENLEAF, A., KURYLEV, Y., LASSAS, M., UHLMANN, G. Electromagnetic wormholes and virtual magnetic monopoles from metamaterials. *Physical Review Letters*, 2007, vol. 99, no. 18, p. 183901.

[7] RAHM, M., ROBERTS, D. A., PENDRY, J. B., SMITH, D. R. Transformation-optical design of adaptive beam bends and beam expanders. *Optics Express*, 2008, vol. 16, no. 15, p. 11555-11567.

[8] RAHM, M., CUMMER, S. A., SCHURIG, D., PENDRY, J. B., SMITH, D. R. Optical design of reflectionless complex media by finite embedded coordinate transformations *Physical Review Letters*, 2008, vol. 100, no. 6, p. 063903.

[9] LIN, L., WANG, W., CUI, J., DU, C., LUO, X. Design of electromagnetic refractor and phase transformer using coordinate transformation theory *Optics Express*, 2008, vol. 16, no. 10, p. 6815-6821.

[10] HUANGFU, J., XI, S., KONG, F., ZHANG, J., CHEN, H., WANG, D., WU, B.-I., RAN, L., KONG, J. A. Application of coordinate transformation in bent waveguide *Journal of Applied Physics*, 2008, vol. 104, no. 1, p. 014502.

[11] TICHIT, P.-H., BUROKUR, S. N., DE LUSTRAC, A. Waveguide taper engineering using coordinate transformation technology *Optics Express*, 2010, vol. 18, no. 2, p. 767-772.

[12] JIANG, W. X., CUI, T. J., MA, H. F., YANG, X. M., CHENG, Q. Layered high-gain lens antennas via discrete optical transformation *Applied Physics Letters*, 2008, vol. 93, no. 22, p. 221906.

[13] MEI, Z. L., BAI, J., NIU, T. M., CUI, T. J. A Planar focusing antenna design using quasi-conformal mapping. *Progress In Electromagnetics Research M*, 2010, vol. 13, p. 261-273.

[14] JIANG, Z. H., GREGORY, M. D., WERNER, D. H. Experimental demonstration of a broadband transformation optics lens for highly directive multibeam emission. *Physical Review B*, 2011, vol. 84, no. 16, p. 165111.

[15] GARCIA-MECA, C., MARTINEZ, A., LEONHARDT, U. Engineering antenna radiation patterns via quasi-conformal mappings. *Optics Express*, 2011, vol. 19, no. 24, p. 23743-23750.

[16] MA, Y. G., ONG, C. K., TYC, T., LEONHARDT, U. An omnidirectional retroreflector based on the transmutation of dielectric singularities. *Nature Materials*, 2009, vol. 8, no. 8, p. 639-642.

[17] TYC, T., LEONHARDT, U. Transmutation of singularities in optical instruments. *New Journal of Physics*, 2008, vol. 10, no. 11, p. 115038.

[18] KUNDTZ, N., SMITH, D. R. Extreme-angle broadband metamaterial lens. *Nature Materials*, 2010, vol. 9, no. 2, p. 129-132.

[19] LIER, E., WERNER, D. H., SCARBOROUGH, C. P., WU, Q., BOSSARD, J. A. An octave-bandwidth negligible-loss radiofrequency metamaterial. *Nature Materials*, 2011, vol. 10, no. 3, p. 216-222.

[20] LUO, Y., ZHANG, J., RAN, L., CHEN, H., JONG, J. A. Controlling the emission of electromagnetic source. In *Progress In Electromagnetics Research Symposium Online*, 2008, vol. 4, no. 7, p. 795-800.

[21] ALLEN, J., KUNDTZ, N., ROBERTS, D. A., CUMMER, S. A., SMITH, D. R. Electromagnetic source transformations using superellipse equations. *Applied Physics Letters*, 2009, vol. 94, no. 19, p. 194101.

[22] POPA, B. I., ALLEN, J., CUMMER, S. A. Conformal array design with transformation electromagnetics. *Applied Physics Letters*, 2009, vol. 94, no. 24, p. 244102.

[23] TICHIT, P.-H., BUROKUR, S. N., DE LUSTRAC, A. Ultradirective antenna via transformation optics. *Journal of Applied Physics*, 2009, vol. 105, no. 10, p. 104912.

[24] TICHIT, P.-H., BUROKUR, S. N., GERMAIN, D., DE LUSTRAC, A. Design and experimental demonstration of a high-directive emission with transformation optics. *Physical Review B*, 2011, vol. 83, no. 15, p. 155108.

[25] TICHIT, P.-H., BUROKUR, S. N., GERMAIN, D., DE LUSTRAC, A. Coordinate transformation based ultra-directive emission. *Electronics Letters*, 2011, vol. 47, no. 10, p. 580-582.

[26] WU, X., TICHIT, P.-H., BUROKUR, S. N., KIROUANE, S., SELLIER, A., DE LUSTRAC, A. Numerical and experimental demonstration of a coordinate transformation-based azimuthal directive emission. *Microwave and Optical Technology Letters*, 2012, vol. 54, no. 11, p. 2536-2540.

[27] TICHIT, P.-H., BUROKUR, S. N., DE LUSTRAC, A. Transformation media producing quasi-perfect isotropic emission. *Optics Express*, 2011, vol. 19, no. 21, p. 20551-20556.

[28] PENDRY, J. B., HOLDEN, A. J., ROBBINS, D. J., STEWART, W. J. Magnetism from conductors and enhanced non-linear phenomena. *IEEE Transactions on Microwave Theory and Techniques,* 1999, . vol. 47, no. 11, p. 2075-2084.

[29] SCHURIG, D., MOCK, J. J., SMITH, D. R. Electric-field-coupled resonators for negative permittivity metamaterials. *Applied Physics Letters*, 2006, vol. 88, no. 4, p. 041109.

[30] NICOLSON, A. M., ROSS, G. F. Measurement of the intrinsic properties of materials by time-domain techniques. *IEEE Transactions on Instrumentation and Measurement*, 1970, vol. 19, no. 4, p. 377-382.

About Authors ...

Paul-Henri TICHIT received the DEA (Master) degree in Theoretical Physics from the University of Blaise Pascal, Clermont Ferrand, France, in 2007. In 2012, he received the Ph.D. degree from the Institut d'Electronique Fondamentale (IEF) - University of Paris Sud 11, France. His Ph.D. research works dealt with the techniques of transformations optics and the application of this methodology to design new electromagnetic devices through the use of metamaterials. He is actually pursuing his research on source transformations as a post-doctoral fellow at the IEF.

Shah Nawaz BUROKUR was born in Mauritius in 1978. He received the DEA (Master) degree in Microwave Engineering from the University of Rennes 1, France, in 2002. In 2005, he received the Ph.D. degree from the University of Nantes, France. His Ph.D. research works dealt with the applications of split ring resonators (SRRs) to microwave devices and antennas. He is actually an Associate Professor at the University of Paris Ouest and carries his research activities at the IEF. His current research interests are in the areas of microwave and applications of periodic structures, complex media, metamaterials and metasurfaces, in the analysis of integrated planar and conformal circuits and antennas. He has published more than 30 papers in scientific journals and holds 1 patent on a metamaterial-based antenna. Dr. Burokur has been the recipient of the Young Scientist Award, presented by the Union Radio-Scientifique Internationale (URSI) Commission B, in 2005. He serves as reviewer of the *IET Microwaves, Antennas and Propagation* and *Electronics Letters* and also the *Journal of Electromagnetic Waves and Applications*.

André de LUSTRAC received the Ph.D. degree in Electrical Engineering in the microwave domain from the Institut d'Electronique Fondamentale (IEF) - University of Paris Sud 11 on Josephson logic devices in 1986. From 1989 to 1992 he was an assistant professor at the Institute of Technology of Cachan, France. He is currently full professor at the University of Paris 10, France. From 2002 to 2007 he was the director of the SITEC department of the University of Paris 10. He has published more than 100 papers in journals and international conferences in the areas of the applications of the superconducting Josephson junctions in digital circuits, the simulation methods of high frequency III-V transistors (HEMT) and quantum circuits, and last but not least, on photonic band gap materials and metamaterials in the microwave and optical domains. He is actually the Head of the Institut d'Electronique Fondamentale, where he explores the physics and the applications of these materials in telecoms and aeronautics. From 2006 to 2012, he has been a scientific adviser of the General Direction of Research and Innovation of the French Ministry of Research and Higher Education.